Empirical tornado resilience model for light-framed wood residential buildings

Justin B. Nevill, Franklin T. Lombardo

Abstract:

An empirical tornado resilience model based on structural functionality, a metric with clearly defined physical states, is developed for light-framed wood residential buildings using field observations of damage and recovery following the February 2017 tornado in Naplate, IL. The resilience model is composed of independent damage and recovery models that serve as a complete resilience model for residential buildings measured with the metric of structural functionality. Structural functionality is the most basic function of a building, the ability to safely provide shelter, and includes both the structural system and the building envelope. This model may be integrated into external resilience models that include measurements of other functionality components, such as lifeline services and building services, to construct a model of total functionality that includes all functionality components necessary for occupancy. The empirical tornado resilience model for light-framed wood residential buildings is an observation-based resilience model for residential buildings subject to tornado damage. It addresses the overlapping critical research needs for studies of tornado hazard, studies of residential resilience, and studies that provide a basis for validation, without replicating the existing body of resilience analysis frameworks. The included analysis using the high resolution of the structural functionality scale indicators of structural functionality for wind-damaged structures reveals that some buildings trend toward zero functionality (demolition) during community-level recovery and that clear differences exist in the recovery behavior of buildings with similar post-storm structural functionality. Exponential structural functionality recovery functions are found to be

appropriate for most levels of damage. Heavily damaged buildings are observed to follow a normal/s-shaped recovery.

1. Introduction

Resilience research holds the promise of improving outcomes of natural and anthropogenic disasters by guiding decision makers and researchers. Resilience studies are designed to guide decision makers (both property owners and policy makers) to strategically adopt existing structural and procedural improvements to reduce the impact of disasters and reduce recovery times [1, 2]. Resilience research guides the research community by revealing the aspects of a structure, system, or community where research progress can have the greatest benefit to society. The impetus for the current study is to improve the overall accuracy of tornado resilience analysis by developing an observation-based model built with minimal assumptions. Ideally, this observation-based model will increase decision makers' confidence in the results of future resilience analyses and encourage the adoption of structural improvements and policy changes that will reduce the immediate and long-term impact of tornado occurrence.

1.1. Resilience Definitions

Despite many variations on the definition of resilience offered in civil engineering research, it is indisputable that resilience is the ability of an individual, system, or community to resist disruption and quickly recover from a disruptive event to a desirable state of functionality [3, 4]. In civil engineering, the community may be a town, state, or nation; the systems are commonly lifeline systems such as power distribution networks, transportation networks, and water supply networks; and individuals are typically single buildings or groups of buildings with a single owner or manager. The disruptive event is commonly assumed to be a natural hazard, but disruptions from anthropogenic disasters, environmental stresses, and economic instabilities are equally valid when discussing resilience. The concept of resilience was introduced to civil engineering to account for both the immediate consequences of a hazard and the near-term consequences related to the rate/duration of recovery. In civil engineering resilience, recovery is the process of activities required to resume normal function of the individual, system, and/or community. The recovery period is the duration of time required to resume normal function, or the arbitrary window of time over which the recovery process is evaluated — depending on the requirements of the particular study.

Resilience can be considered the logical extension of the risk framework to include recovery, where risk is the probability of undesirable consequences. Improvements/degradations that increase/decrease resilience can act in three major ways: by changing the amount of damage done during the disaster (any disruptive event), by changing the rate of repairs/recovery, or by changing the final level of functionality after recovery. Koliou et al [2] provides an excellent review and brief history of the contemporaneous state of resilience research in civil engineering.

Resilience, and each component of resilience, is defined in terms of functionality. Functionality is most simply defined as the ability to serve the intended purpose [5]. Functionality requirements for buildings will vary based on the occupancy but can generally be described as the ability to safely shelter the occupants and allow intended activities (occupancy). Allowing occupancy requires structural functionality, lifeline services, and building services (e.g. indoor environment controls, lighting, elevators) — each occupancy class will have specific requirements. The structural functionality, lifeline services functionality, and building services functionality are individual components of the total functionality of a building. Structural functionality is the ability of a building to safely provide shelter [6] and is fundamental to the total functionality of any building; every building must provide shelter and be safe to enter to be fully functional, regardless of the occupancy.

Therefore, resilience is increased by preserving functionality and increasing the restored functionality. Resilience studies often include a target functionality level, a target recovery time, or both to determine the period of time during which changes in functionality are related to the disaster and recovery process. It is important that functionality not be confounded with financial value because damage that leads to costly repairs of finishing materials and other non-critical items can be associated with inconsequential changes in functionality and resilience. When financial measures are desired for profitability/loss-based decision making, resilience analysis provides an excellent mechanism for predicting physical damage states and estimating downtime[7].

1.2. Resilience Quantification

It is advantageous to quantize resilience for the purpose of comparing potential improvements to buildings, infrastructure, and policy to each other and to the existing baseline resilience. Resilience is often quantized as the integral of a measure of functionality over a period of time following a disaster [7, 8]. A resilience model must include two primary components: one to model the degradation of functionality (damage) and one to model the increase of functionality after the event (recovery). Each of these may have multiple subcomponents to account for any combination of social, physical, political, and economic parameters.

Many conceptual resilience models adopt a prescribed recovery behavior as part of a deterministic model or basis for stochastic recovery rates. Fig. 1 represents four of the most common models [9]. Conceptual frameworks for resilience can be, and have been, developed without defining specific metrics of functionality because the basic mathematics and relationships do not rely on a specific metric. Purely conceptual resilience models often fail to match the physics of the recovery process [10] and should not be considered as accurately predicting resilience unless they are validated with observations [2]. Lin and Wang [11] develop a recovery model that eschews deterministic recovery functions in favor of a transition-matrix where individual buildings have unique, stochastically driven recovery paths, that are combined to describe the recovery of the community building portfolio. Application of these conceptual frameworks requires that functionality be clearly defined and given an unambiguous metric, just as all measures (e.g. time, length, mass) require an unambiguous metric (e.g. second, meter, kilogram) for application.

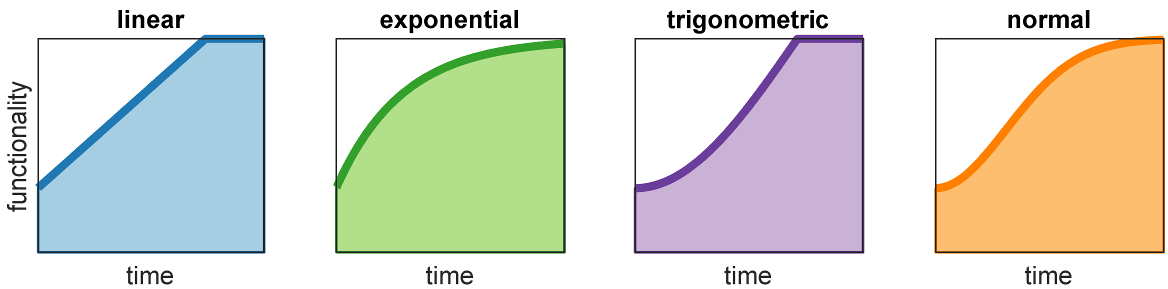

Fig. 1 Common recovery model function shapes.

Resilience research to date has focused primarily on lifeline buildings and systems, where functionality metrics are easily defined and a specific set of formal plans and policy can dominate changes to the resilience [17, 18, 19, 2]. The functionality of buildings has been less thoroughly studied than that of lifeline systems [2, 12] and the appropriate metric for use is less clear. The functionality of service-oriented buildings may be measured with a metric based on the occupancy. For example, the functionality of a hospital may be measured with the metric of percentage of hospital beds available [13] or the metric of average emergency room waiting time

[14, 15]. An unambiguous metric for residential building functionality is more elusive, and resilience of residential buildings has not been sufficiently studied, despite the critical role these buildings play in communities [2].

1.3. Resilience and functionality of residential buildings

The recovery of residential buildings is particularly difficult to predict because it is controlled by a combination of homeowner decisions, insurance policy, local and regional government policy, and a broad set of socioeconomic influences [16-18]. Sutley and Hamideh [18] present a conceptual framework designed specifically for residential buildings which describes many of the social, economic, and policy factors that influence residential building recovery and provides a framework for including these factors in resilience analysis, a step toward addressing inequalities in housing recovery. The two most commonly-used metrics for building condition are the safety metrics of ATC 20 by Applied Technology Council [19] and the damage states of HAZUS-MH [20] — however, neither of these measures functionality or is intended for use in resilience analysis. ATC 20 is only intended to rate the safety of buildings immediately following an earthquake [19]. HAZUS-MH is a risk-assessment tool that predicts recovery time based on financial loss (percentage of total value) at a building-component-level resolution; the damage states of HAZUS-MH are only intended for summary representation of the aggregate damage [21]. As previously discussed, financial loss is not directly proportional to functionality. Many damage models used for resilience analysis use a metric very similar to the damage states of HAZUS-MH [22-24]. Unfortunately, these models focus on physical damage instead of lost functionality and inherit the low resolution of HAZUS-MH damage states, essentially ignoring the significant difference in functionality, recovery time, and recovery behavior that exists among buildings within “severe damage” and “destruction” HAZUS-MH classifications [6, 21].

The existing body of residential resilience primarily relies on indirect measurements of functionality aggregated across many residences [12, 17, 25-27].

The total functionality of a building can be unambiguously measured as a combination of functionality components: structural functionality, lifeline services functionality, and building services functionality. To be fully functional, any building requires full structural functionality and full functionality of all required lifeline services and building services. Lifeline services functionality can be unambiguously measured as described above, building services functionality can be similarly measured as the percentage of the building served or percentage of equipment operable, and structural functionality can be unambiguously measured with the structural functionality scale [6]. Structural functionality of a building includes the structural system and the building envelope, both of which are required for the building to safely provide shelter. As such, structural functionality is the portion of total building functionality that is native to the building itself while lifeline services are largely external to the building and building services are provided by equipment added to/included with the building. The structural functionality scale [6] is hazard agnostic and can be defined for any construction type or occupancy with the development of appropriate structural functionality indicators. Table 1 includes indicators of structural functionality for wind-damaged residences, including structural functionality increments for recovery.

The existing body of residential building resilience research focuses primarily on earthquake and hurricane damage, despite the large impact tornado damage has on non-coastal communities in the US. Overall, there is a dearth of research directly applicable to the resilience of residential buildings damaged by tornadoes [2].

Table 1. Structural functionality indicators for wind-damaged buildings (Adapted from [6])

Functionality rating	Cover missing	Sheathing penetrations		Roof/wall structure	Repair indicators
		Size	Coverage		
1.0	0	0		No damage	No repairs required
0.9	<10%	0		No damage	Cover>90% complete
0.8	10%–25%	< 0.3mx0.3m	<25%	No damage	Cover 50%–90% complete
0.7	>25%	< 0.3mx0.3m (or) 0.3x0.3 to 1mx2m	25%-50% (or) 1 side	No damage	Sheathing complete, cover <50% complete
0.6	n/a	< 0.3mx0.3m (or) 0.3x0.3 to 1mx2m	>50% (or) >1 side	No damage	>80% of sheathing complete
0.5	n/a	>1mx2m	1–3 penetrations	No damage	25%–80% of sheathing complete
0.4	n/a	>1mx2m	>3 penetrations	Isolated damage, no risk of primary structure collapse	Wall and roof frames complete
0.3	n/a	n/a	n/a	Risk of localized collapse	Wall frames complete
0.2	n/a	n/a	n/a	<25% area at risk of collapse (or) roof destroyed w/ walls intact	Walls partially framed
0.1	n/a	n/a	n/a	25%-50% area at risk of collapse (or) damage to >50% of structural members	Foundation prepared
0.0	n/a	n/a	n/a	>50% at risk of collapse (or) no salvageable structure	No progress past demolition

1.4. Windstorm resilience of residential buildings

Damaging winds originate from many types of weather events. The damage from tropical cyclones (hurricanes), tornadoes, thunderstorms, or synoptic weather systems is often considered collectively as windstorm damage [28]. However, the properties of the wind generated by these storms is dissimilar, as are the level and presence of secondary hazards (e.g. rain, storm surge, hail). The differences in wind loads and damage from wind generated by different storm systems is an unanswered question [29], but the inclusion/exclusion of water intrusion as part of a wind damage model has known considerable consequences. Hurricane resilience and tornado resilience both include damage from extreme wind speeds, but the resilience research from one cannot be directly applied to the other.

The majority of windstorm resilience research that has been conducted focuses on hurricanes. Zhang and Peacock [17] uses data from Miami-Dade County property tax appraisal and census data as a proxy for residential building functionality following Hurricane Andrew. Tokgoz and Gheorghe [9] builds a conceptual model of residential resilience to hurricane damage. The concepts and framework presented in these studies could be adapted to tornado resilience models with the understanding that the damage and recovery models will be different.

Existing tornado resilience research for individual residential structures primarily relies on analytical fragility models to determine the level of damage and conceptual recovery models to determine the rate of recovery [26, 30, 31]. Multiple analytical fragility models for damage from hurricane and tornado winds have been developed for light-framed wood structures [24, 32]. Physics-based methods, where simulated loads are applied to finite element models, have also been used to develop fragility models [33]. Few fragility models for wind have been calibrated with full-scale measurements and observations. Roueche, Lombardo, and Prevatt developed empirical fragility models for residences [34] and the uncertainty in these fragilities [35] based on observations of tornado damage.

Few studies address recovery from tornado damage [2, 12]. The most complete resilience model for light-framed wood residential structures currently available is developed in multiple publications by members of the Center of Excellence for Risk-Based Community Resilience Planning, some in the support of the Interdependent Networked Community Resilience modeling Environment (IN-CORE) [36]. Combined, these publications present fragility models and recovery functions for nineteen archetypal buildings, a minimum community building portfolio [30]. Koliou and van de Lindt [37] propose a probabilistic framework for considering the repair time and direct cost fragilities for buildings subject to tornado hazards. The light-framed wood residential building archetypes rely on the fragilities presented in 2018 by Masoomi and van de Lindt [24] and repair times estimated by the US Federal Emergency Management Association (FEMA) in a HAZUS technical manual (reference incomplete). The repair times likely rely on those estimated in the Hurricane Model [21] because no tornado component was developed for HAZUS at the time of publication. Koliou and van de Lindt suggest a set of functionality ratings (25% reduction in functionality for each increasing damage state) for each of the four damage states with the caveat that the relationship between damage and functionality is beyond the scope of the publication. Damage and recovery data collected from Joplin, MO after the 2011 tornado is used as validation for tornado components of the damage models of the IN-CORE resilience model [23, 38]. Validation of the IN-CORE tornado recovery model is ongoing [36].

Overall, the existing body of tornado resilience research for light-framed wood residential buildings includes both analytical and empirical fragility models that were developed to describe damage without consideration of building functionality; conceptual recovery models which use either damage or other functionality surrogates; and a robust collection of resilience frameworks that could be applied to tornado resilience. Koliou and van de Lindt [37] presents the only resilience framework presented here that is designed specifically for tornado hazard but most resilience frameworks can be adapted to any hazard if the appropriate hazard magnitude estimates, damage model(s), and recovery model(s) are available. No existing publication develops the functionality-based tornado damage and recovery models necessary for resilience analysis of light-framed wood residential buildings. Furthermore, the existing body of windstorm resilience research includes no recovery models which have been validated with experiments or observations; the accuracy of resilience analysis results is uncertain without empirical studies of resilience and validation of conceptual resilience models [4].

2. Model development

The primary focus of this work is to use observations to model (1) functionality lost due to tornado damage and (2) the following recovery for light-framed wood residential buildings (single-family one- and two-story residential buildings of standard construction). The empirical model of tornado resilience for light-framed residential structures developed here is composed of independent damage and recovery models. The damage and recovery models can be used as a complete resilience model for light-framed wood residential structures and/or incorporated into existing or future community-level resilience models. The empirical models are developed as an alternative to the existing body of conceptual damage and recovery models. Ideally, it will also serve as a benchmark for validating existing and future conceptual resilience models. As this resilience model is based on observations with minimal assumptions, it can be shown to be consistent with its own empirical basis. This observation-based resilience model for residential buildings subject to tornado damage fills overlapping critical research needs for studies of tornado hazard, studies of residential resilience, and studies that provide a basis for validation.

Empirical models have unavoidable limitations: they can only be guaranteed to be consistent with scenarios similar to their empirical basis. Without extrapolation, the model developed here is limited to a modest range of tornado wind speeds and residential buildings similar to those present at the time of the basis event. These limitations are further discussed in Sec. 4.

The measurement basis of this study is the structural functionality scale and indicators of structural functionality for wind-damaged buildings [6]. This scale is unique in providing a direct measure of functionality. Structural functionality is the most fundamental component of a building, the ability to safely provide shelter, but is only one component of the total functionality required to enable the intended occupancy. For most light-framed residential buildings, the lifeline services of external power, fresh water, sanitary sewer, and transportation access as well as the building services heating/cooling and food storage/preparation would typically be required for full total functionality. However, these lifeline services and building services are controlled by different recovery mechanisms and will not be considered in this study. This empirical model uses observations of the building to measure structural functionality, but the structural functionality metric can also be implemented numerically in simulations.

Tornado damage is commonly measured in terms of the Enhanced Fujita Scale (EF-Scale) where wind speeds estimated from damage to one-story and two-story light-framed residential buildings are covered as Damage Indicator 2 with ten Degree of Damage ratings (EF-Scale DOD) [39]. EF-Scale Damage Indicator 2 DOD ratings are included in this study to allow comparison and compatibility with existing and future work by others where EF-Scale DOD is the primary metric.

2.1. Data Collection

The empirical basis of the resilience model for tornado damage is data collected during field surveys following the 28 February 2017 tornado in Naplate, IL. The National Weather Service rated the tornado as an EF-3 on the EF-Scale with estimated peak wind speeds of 70 m/s (155 mph), total path length of 18.5 km (11.5 miles), maximum damage width of 0.73 km (0.45 miles), and a duration under 20 minutes [40]. The storm resulted in 14 injuries, 2 deaths, and damaged most of the buildings in the village of Naplate.

The Wind Engineering Research Laboratory at The University of Illinois at Urbana-Champaign (UIUC WindLab) surveyed the initial damage caused by the tornado and the recovery of residential wood-framed buildings in the community. UIUC WindLab conducted five surveys of the community, occurring at 2 days after the tornado, 111 days after the tornado, 168 days after the tornado, 377 days after the tornado, and 728 days after the tornado. After a recovery period of two years, one building remained significantly damaged, and nine buildings were demolished without replacement. The field campaign was ended after two years because only one of the 151 buildings was clearly in the process of repairing damage from the tornado. New construction or improvements following the two-year period would not clearly be related to tornado recovery.

During each survey, UIUC WindLab researchers photographed all affected buildings and recorded observations of the condition of the buildings. During the initial (day 2) survey and the second (day 111) survey, additional data was collected regarding the damage to trees, street signs, traffic signs, and distribution poles for wind speed estimation. Researchers recorded the EF-Scale DOD of all light-framed wood residences (EF Damage Indicator 2) during the initial survey. The color fields in Fig. 2 represent the estimated maximum wind speed experienced during the tornado event; buildings surveyed and their respective EF-Scale DOD are represented with squares. The analysis that follows includes the 151 buildings surveyed in this campaign and

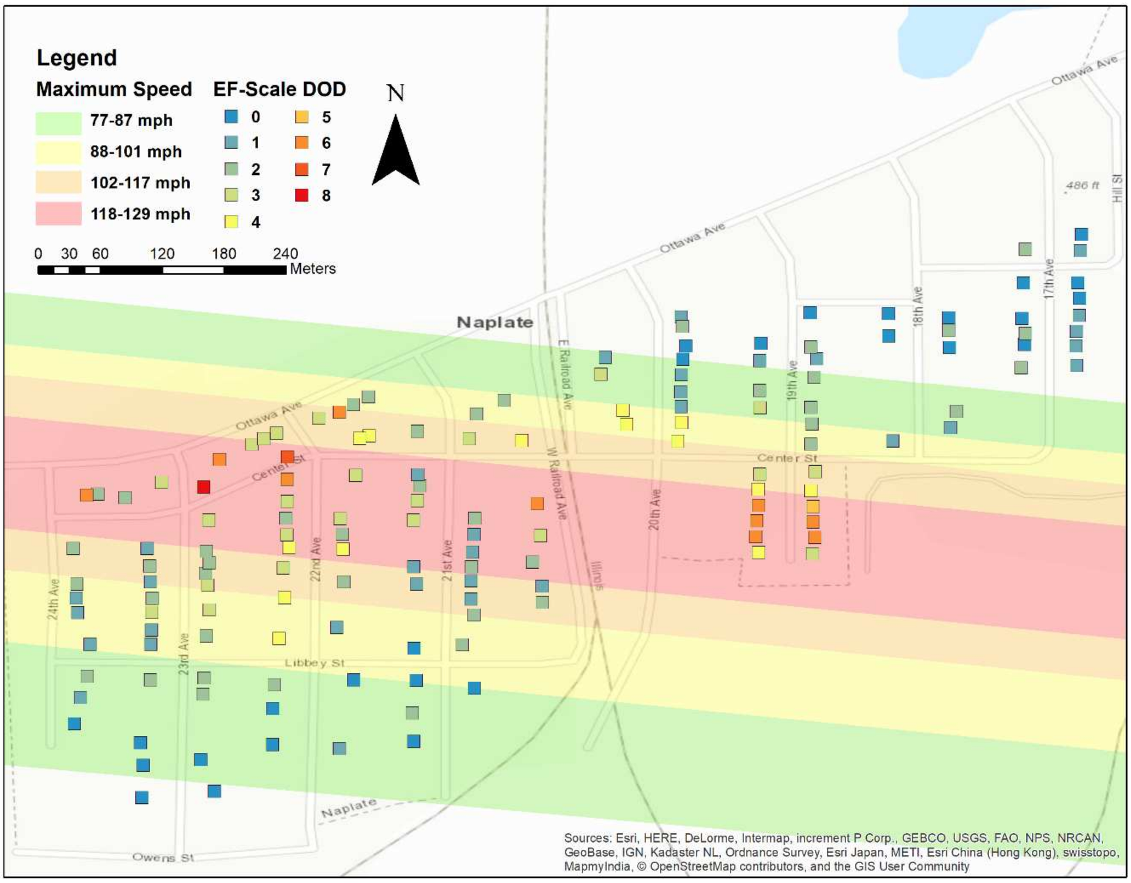

Fig. 2 Survey region of Naplate, Illinois with estimated wind field and EF scale Degree of Damage (DOD). Image by Daniel M. Rhee.

identified in Fig. 2.

2.2. Damage Observations

Two independent measures of damage comprise the damage observations: structural functionality measurements, where damage is measured as a reduction in the ability of the building to serve as a safe shelter, and EF Scale DOD ratings, which use damage indicators to estimate wind speeds. These two measures are not perfectly correlated because they represent fundamentally different quantities (wind speed and structural functionality) [6]. Additionally, the structural functionality scale includes decreases in functionality that result from secondary wind hazards, such as damage caused by wind-felled trees striking a building. The EF Scale estimates do not include secondary wind hazards because such damage is not an indicator of wind speed. Resilience fundamentally relies on measures of functionality; EF-Scale DOD ratings are only included to allow comparisons with existing damage surveys and models. UIUC WindLab researchers determined the two measures (EF-Scale DOD and structural functionality rating) independently for each of the 151 buildings in this study.

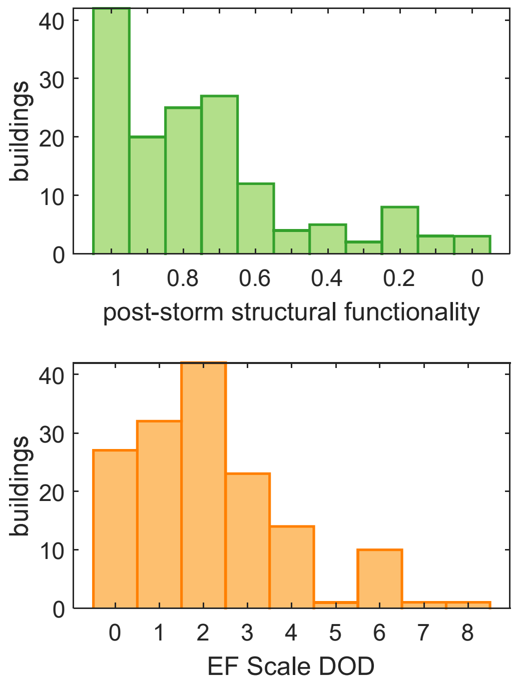

Fig. 3 Histograms of observed post-storm structural functionality and EF Scale DOD

Fig. 3 shows the distribution of EF-Scale DODs (DOD #) and post-storm structural functionality (SF #) for affected buildings. The two distributions have similar overall behavior with a peak at a state of moderate damage and decreasing totals in higher damage states. Two clear differences are the lowest damage state (highest functionality) where some buildings were observed with visible signs of wind damage that did not reduce functionality (such as minimal scouring of paint on walls), and DOD 5 “entire house shifts off foundation” [39] which corresponds to the lowest structural functionality state, SF 0.

	Post-storm Structural Functionality											
EF-Scale DOD	1	0.9	0.8	0.7	0.6	0.5	0.4	0.3	0.2	0.1	0	**Sum**
0	23	2		2								**27**
1	17	7	2	6								**32**
2	1	11	19	8		1	1			1		**42**
3			1		10	10	1	1				**23**
4			4	1	2	2	3			1		**14**
5											1	**1**
6								1	8	1		**10**
7											1	**1**
8											1	**1**
Sum	**42**	**20**	**25**	**27**	**12**	**4**	**5**	**2**	**8**	**3**	**3**	**151**

Table 2. Distribution of combined EF-Scale and post-storm structural functionality

Breakdown of the number of buildings at each combined EF-Scale DOD and structural functionality rating reveal the expected trend (Table 2). Specific outliers in the trend between EF-Scale DOD and structural functionality primarily reflect levels of damage that reduce functionality but do not increase the EF-Scale DOD. Two of the DOD 2 buildings with structural functionality below SF 0.7 have secondary wind damage from tree impact; the third has a localized structural damage that is not indicative of higher wind speeds. The single building rated at DOD 4 and structural functionality SF 0.1 does not meet the criteria of higher EF-Scale DOD ratings, but at least 25% of the habitable area is at risk of collapse (Fig. 4).

Fig. 4. DOD 4 building in Naplate, IL with post-storm structural functionality of SF 0.1.

Some of the buildings with low EF-Scale DOD ratings, especially DOD 0 and DOD 1, have structural functionality lower than full functionality due to preexisting conditions unrelated to the February 2017 tornado. These preexisting conditions include deferred maintenance and ongoing renovations. Preexisting conditions were primarily identified visually, information volunteered by residents was included where possible. Deferred maintenance primarily included degraded roofing and missing fascia or building trim, all of which are easy to identify; these buildings were all in a usable state. Two DOD 0 residences were determined to have had siding removed before the tornado because no siding was present when adjacent buildings had superficial damage, the buildings themselves had no damage to shingle roofing, and both buildings were covered with aging house wrap.

2.3. Structural Functionality Damage Model

The damage model includes two components: an empirical structural functionality fragility model for light-framed wood buildings and suggested conversions from EF-Scale DOD measures to structural functionality states. Rhee and Lombardo [41] includes EF-Scale DOD fragilities based on this dataset. This damage model focuses on structural functionality because it is a true metric of building resilience.

The empirical structural functionality fragility model in Fig. 5 provides a convenient method for predicting the post-storm structural functionality. The assumption that exceedance observations are members of a binary distribution with probabilities normally distributed in relation to the natural log of the wind speed provides the basis for empirical fragilities, as established for

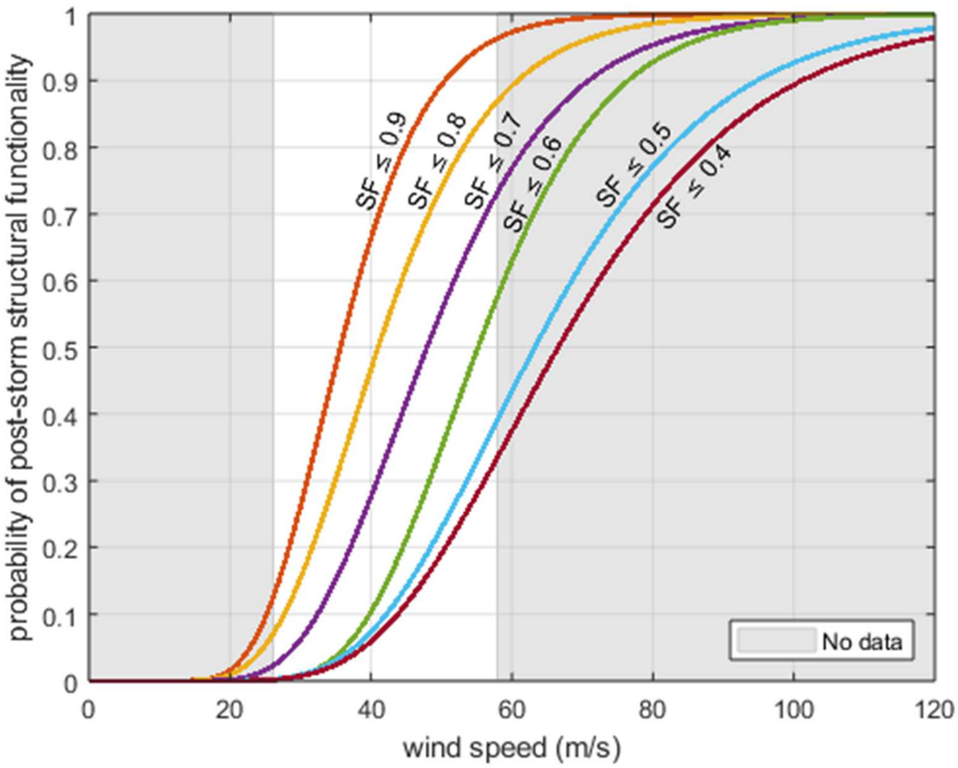

Fig. 5. Empirical structural functionality fragility for SF 0.4 through SF 0.9.

seismic fragilities [42] and previously used for tornado fragilities [34, 41]. This method relies on accurate estimates of the peak wind speeds at each of the damage observations. The wind field developed in Rhee and Lombardo [41] using patterns of tree fall direction provide the peak wind speeds required in this damage analysis (reproduced here in Fig. 2). The maximum estimated peak wind speed for the February 2017 tornado in Naplate is 57.7 m/s (129 mph).

All fragility curves in Fig. 5 have the expected progression of reduced functionality with higher wind speeds. The fragility curves for SF=0.9 through SF=0.6 have similar shape and fairly even spacing. The long tail observed at higher wind speeds in the fragility curves for structural functionality SF=0.5 and SF=0.4 is likely due to the lack of wind speed observations above 60 m/s in this study. Structural functionality fragilities below SF=0.4 are excluded from Fig. 5 because too few observations were present for reliable parameter estimation.

For higher wind speeds and more severe damage, the EF-Scale DOD fragilities based on damage observations in Joplin, MO [34] or analytical methods [24] can supplement the empirical structural functionality fragility model. Table 3 provides a probabilistic conversion from EF-Scale DOD to structural functionality for cases where EF-Scale DOD fragilities are necessary.

Nevill and Lombardo [6] establishes a qualitative relationship between structural functionality and EF-Scale DOD. Any building with EF-Scale DOD of 5, 8, 9, or 10 is either destroyed or at risk of collapse and has a structural functionality of SF 0. An analytical relationship is difficult to establish for other EF-Scale DODs because progressive indicators of wind speed and progressive indicators of reduced structural functionality are not coupled, despite the relationship between higher wind speeds and greater damage. To better establish the relationship between structural functionality and EF-Scale, the structural functionality of all 151 buildings in the dataset are reevaluated to only include reductions in functionality that result from direct wind damage. The values in Table 3 are based on the proportion of structural functionality observations per EF-Scale DOD with indirect and non-wind functionality reductions removed.

	P (functionality | DOD)										
	1	0.9	0.8	0.7	0.6	0.5	0.4	0.3	0.2	0.1	0

EF-Scale DOD											
0	0.85	0.05	0.05	0.05							
1	0.55	0.25	0.1	0.1							
2	0.02	0.34	0.48	0.16							
3				0.45	0.45	0.10					
4			0.28	0.07	0.14	0.14	0.2	0.07	0.06	0.04	
5											1
6								0.1	0.8	0.1	
7									0.25	0.5	0.25
8											1
9											1
10											1

Table 3. Probability of post-storm structural functionality given EF-Scale DOD.

Table 3 reflects the expectation of decreasing structural functionality with increasing EF-Scale DOD, with the exception of DOD 5 “entire house shifts off foundation” [39]. The wide distribution of structural functionality for DOD 4 buildings reflects the wide range of conditions described by “uplift of roof deck and loss of significant cover material (>20%); collapse of chimney; garages doors collapse inward; failure of porch or carport” [39]. In Naplate, buildings rated at DOD 4 include conditions ranging from shingle loss to risk of partial collapse (Fig. 4). The distribution of functionalities for DOD 7 is a purely conceptual estimate due to the lack of buildings rated DOD 7 in the dataset.

A robust damage model must include secondary wind damage that reduces structural functionality, such as damage from wind-felled trees that strike a building. The uncertainty in tree impact for a generic building is too high to be included in building fragility models. To include such representations, a geospatial model of the analysis region can be coupled with tree fragilities [43] and a wind field model with peak speed and direction [41] to connect the probability of tree fall with fall direction and proximity to buildings.

2.4. Structural Functionality Recovery Observations

The structural functionality scale's indicators for wind-damaged buildings during recovery (Table 1) are used to measure the structural functionality of 151 residences over the 2-year observation period [6]. In the recovery process, damage to/deficiencies in the building structural system and building envelope is repaired (on average), resulting in an increase in structural functionality. Some buildings may have permanent or temporary reductions in structural functionality due to full or partial demolition. The recovery indicators describe incremental recovery steps; structural functionality cannot skip states in recovery. Between the five observation points, the structural functionality of each building is linearly interpolated to estimate the duration of each incremental functionality state. For residences where the building is known to be demolished and rebuilt/partially-rebuilt between observations, linear interpolation is extended to provide identical rates of decreasing and increasing structural functionality between observations with a point of zero functionality occurring between observations.

The distributions of observed structural functionality, with interpolated data, are represented in Fig. 6 with residences grouped by the observed EF-Scale DOD. All residences in the groups with EF-Scale DOD 0 through DOD 3 recover toward full structural functionality, SF 1. Within these less-damaged groups, some residences had temporary decreases in functionality resulting from removal of undamaged roofing, siding, or structural members during the recovery process. An obvious outlier exists in the DOD 0 group, where a building with high structural functionality was demolished and rebuilt. Unsolicited anecdotal information explains this phenomenon: the homeowner needed to build a larger residence to accommodate a family member displaced from a different residence damaged by the tornado.

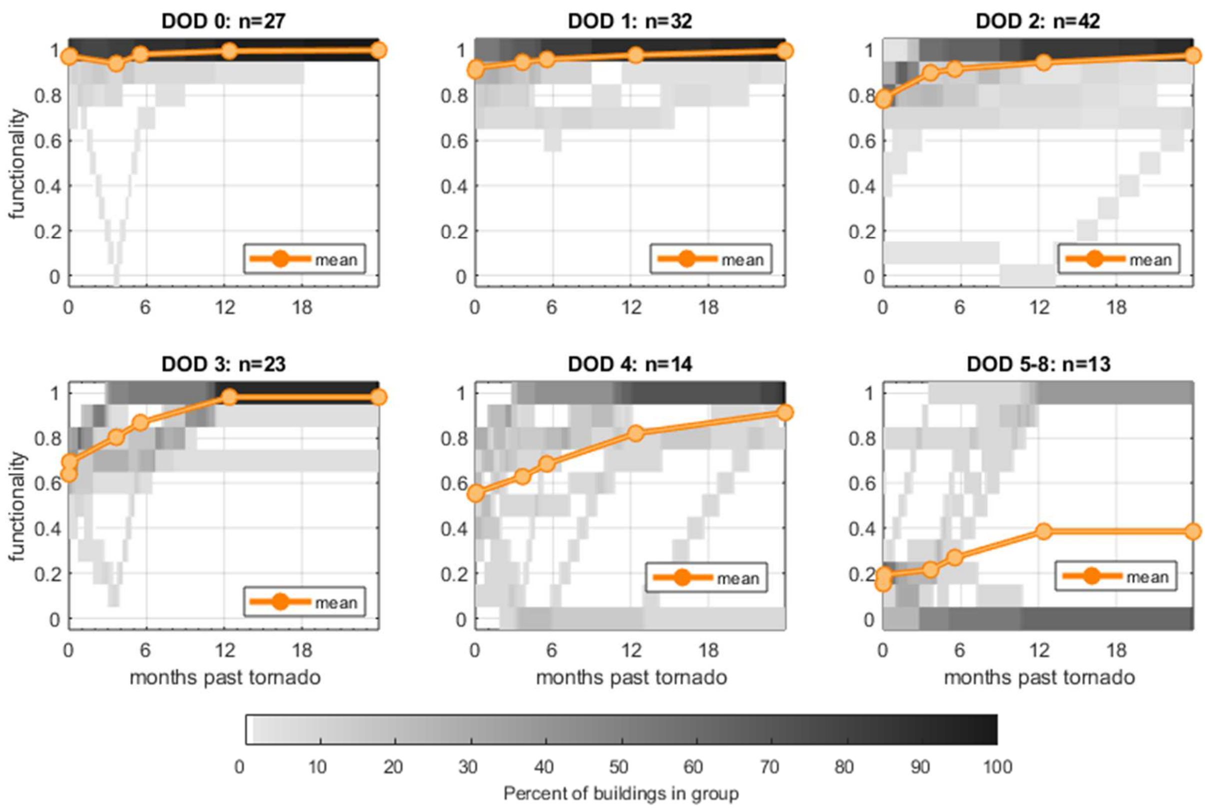

Fig. 6. Distribution and mean of observed recovery of structural functionality with interpolated data, separated by EF Scale DOD.

Unlike the less-damaged buildings, the recovery of residences with EF-Scale DOD 4 through DOD 8 is bifurcated with individual buildings approaching either full functionality or zero functionality (demolished) during the community's recovery process (Fig. 6). Within the more heavily damaged groups, some buildings recover toward full structural functionality while others are demolished and not rebuilt. The field project supporting this research did not include homeowner interviews: the underlying differences in behavior is uncertain. For these groups the mean behavior of the group, represented in orange, trends to a value less than SF 1; this final value is similar to the percentage of buildings in the group that are rebuilt instead of being demolished.

Dividing the residences in two groups based on post-storm structural functionality adds clarity to the disparity in behavior. In Fig. 7, most residences with post-storm structural functionality at or above SF 0.4 recover toward full structural functionality while most buildings with post-storm structural functionality below SF 0.4 are demolished and not rebuilt. The mean behavior of the two groups shows buildings with post-storm functionality SF≥0.4 monotonically increasing in structural functionality on average while those with post-storm functionality SF<0.4

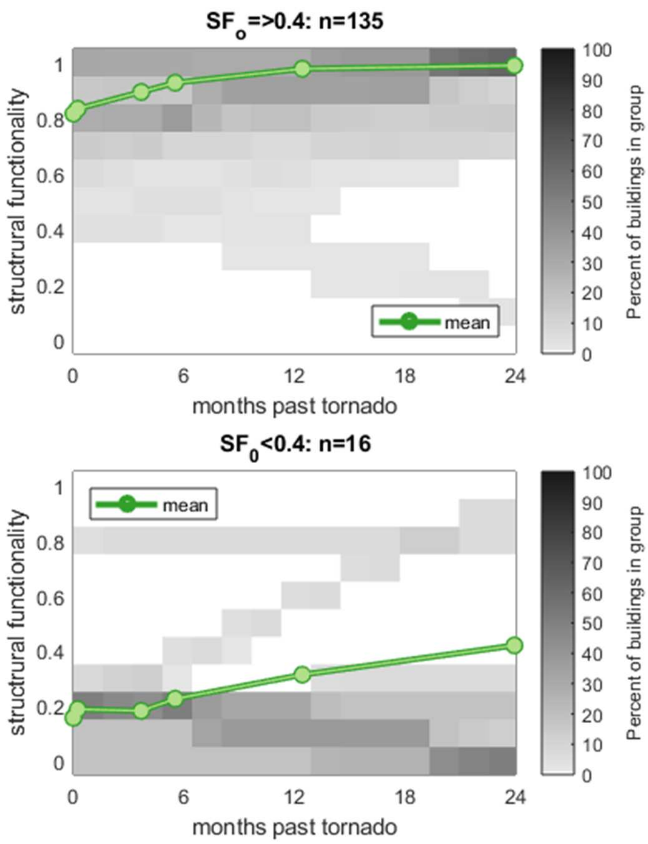

Fig. 7. Distribution and mean of observed recovery of functionality with interpolated data, separated by functionality immediately following tornado.

has an initial decrease/plateau in structural functionality before the mean value increases. This mirrors a division in the structural damage between isolated damage and damage that is more widespread: buildings with SF 0.4 have only isolated damage to individual structural members while buildings with structural functionality SF 0.3 have some risk of localized collapse. The observation that buildings divided into two groups by structural functionality recover more similarly within the groups than buildings divided into six groups by EF-Scale DOD reinforces that the structural functionality scale is a superior predictor of recovery behavior.

2.5. Structural Functionality Recovery Model

Observations of actual recovery, enumerated on an unambiguous scale, provide a sound basis for a recovery model that accurately represents the set of observations and can be trusted to model similar events. Deterministic models cannot accurately represent the observed recovery behavior for individual buildings because they assume the recovery rate is identical for similarly damaged buildings. Unlike deterministic recovery models, a state-transition matrix model captures the behavior where similarly damaged buildings have unique recovery paths. The inclusion of decreasing functionality transitions in the recovery model is necessary to match the observed behavior. This behavior is not explicitly included in most conceptual models, which typically assume monotonically increasing recovery.

A model based on a state-transition matrix retains the uncertainty observed in recovery. To build the transition matrix, the change in structural functionality states for each building between adjacent weeks, including interpolated points described in Sec. 2.4, is recorded as a state change. This change in states includes the dwell transition where structural functionality is unchanged. For any component of the state transition matrix, p_{ij}, the value represents the probability of transitioning from state i to state j at any transition between weekly observations. The probability of transition is calculated as the proportion of transitions from each structural functionality state (Eq. 1). Identical analysis using a daily transition interval does not yield meaningfully different results.

$$P = p_{ij} \equiv \frac{number\ of\ transitions\ fron\ i\ to\ j}{number\ of\ transitions\ from\ i\ to\ any\ state} \qquad (1)$$

The result is a sparse transition matrix with transitions limited to incremental changes – this arises naturally because structural functionality is a continuum and construction, demolition, and repair are necessarily incremental. This methodology is similar to the model developed by Lin and Wang [11] in that both use a state transition matrix. However, Lin and Wang assume that functionality is monotonically increasing and present a conceptual model that allows transition to any higher state while the proposed model allows increasing or decreasing functionality, limits transition to adjacent functionality states, and is based on observations of recovery.

Table 4. Functionality transition matrix values using 1-week transition period

	P(transition)	Future functionality										
		0.0	0.1	0.2	0.3	0.4	0.5	0.6	0.7	0.8	0.9	1.0
Current functionality	0	0.991	0.009									
	0.1	0.105	0.827	0.068								
	0.2		0.083	0.834	0.083							
	0.3			0.111	0.683	0.206						
	0.4				0.090	0.657	0.253					
	0.5					0.052	0.742	0.206				
	0.6						0.029	0.750	0.221			
	0.7							0.004	0.927	0.069		
	0.8								0.003	0.924	0.073	
	0.9									0.003	0.914	0.083
	1										0	1

For any structural functionality state, the transition matrix allows three possible transitions: decrease in structural functionality by ΔSF= - 0.1, no change in structural functionality (ΔSF=0), and increase in structural functionality by ΔSF=0.1. The resulting state-transition matrix is reproduced as Table 4. The transition probabilities for buildings with no remaining structural functionality, SF 0, reflects the low percentage of buildings that recovered from this state. At the other extreme, buildings with full structural functionality have no chance of reduced functionality at the next time step (to the precision represented in the table). Buildings with structural functionality SF 0.1 are more likely to decrease in functionality than increase in functionality, buildings with structural functionality SF 0.2 have an equal chance of increasing or decreasing in functionality for any transition, and buildings with structural functionality between SF 0.3 and SF 0.9 are much more likely to increase in functionality than decrease in functionality. Probabilities on the diagonal reflect the chances that the structural functionality of a building will not change between adjacent weeks. These dwell probabilities are lowest for moderate structural functionality (SF 0.3 to SF 0.6) which can be interpreted as the general behavior of more-rapid recovery for moderate functionalities and decreasing rates of recovery toward the extremes. This matches the observed asymptotic behavior of long-term recovery.

Implementation of the state-transition matrix in a Markov-Chain Monte-Carlo simulation (MCMC) provides realistic stochastic building-level recovery estimates that can be validated with field observations. The probabilities in the state-transition matrix drive the change in structural functionality for each individual building. The overall recovery for a MCMC is determined in an iterative process where each iteration is a weekly change in structural functionality state of each building and the number of iterations matches the duration of consideration defined for the simulation. The results can be aggregated or analyzed individually.

For comparison with the observed recovery, the structural functionality state-transition MCMC was conducted on 151 buildings whose post-storm functionality were the same as those observed for the 151 buildings in Naplate. Each iteration of the MCMC was run for 105 weekly time steps (about 2 years) to capture average behavior and the distribution of possible simulations. The MCMC was run for 10,000 iterations for the discussion in this section. For Sec. 2.6, the MCMC was run using one sample building per initial functionality until convergence (as measured by the maximum relative error across all buildings and time steps with the strict threshold 1e-5). The difference in the resulting mean values is not visually discernable.

Fig. 8 provides a comparison between the simulated recovery and the observed recovery for each EF-Scale DOD group. For each of the EF-Scale DOD groups, the observed mean recovery lies primarily within the 95% interval. Exceptions are the mean recovery of DOD 0 buildings at the third observation point (4 weeks) where an undamaged building was demolished and rebuilt, as previously discussed, and the second observation point (2 days) for several groups where early increases in structural functionality due to temporary stopgap repairs are poorly captured by the model. Overall behavior for the EF-Scale DOD groups shows exponential-like recovery for all but the most heavily damaged buildings. Moderately damaged EF-Scale DOD groups have an exponential-like recovery that trends toward a level less than full structural functionality. Some buildings in this model simulation are not fully repaired within the 2-year recovery period.

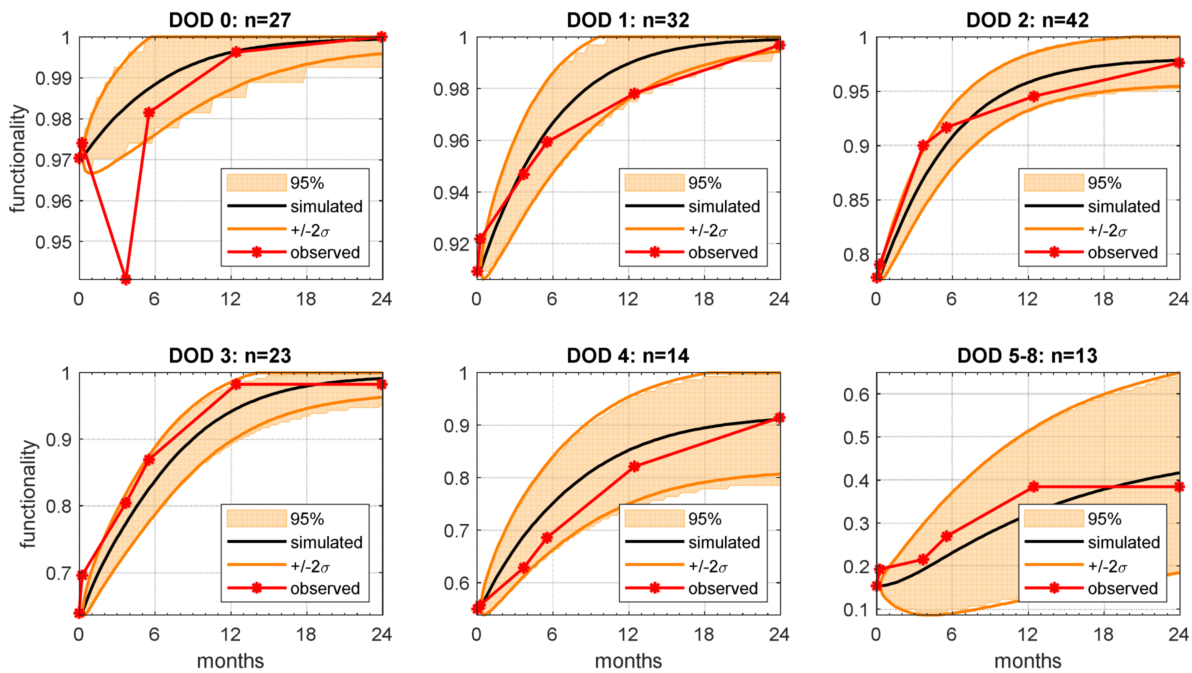

Fig. 8. Distribution and mean of simulated recovery of structural functionality with mean observed structural functionality, separated by EF Scale DOD.

The distribution of the mean simulated recovery of all 151 buildings in the dataset includes five of the six mean observed structural functionality point for Naplate within two standard deviations (Fig. 9, top). While this metric is not especially meaningful and is highly sensitive to the geographic boundary of the field sample, the comparison establishes that the simulated recovery behaves similarly to the mean recovery behavior of the community, not just the recovery of individual EF-Scale DOD groups.

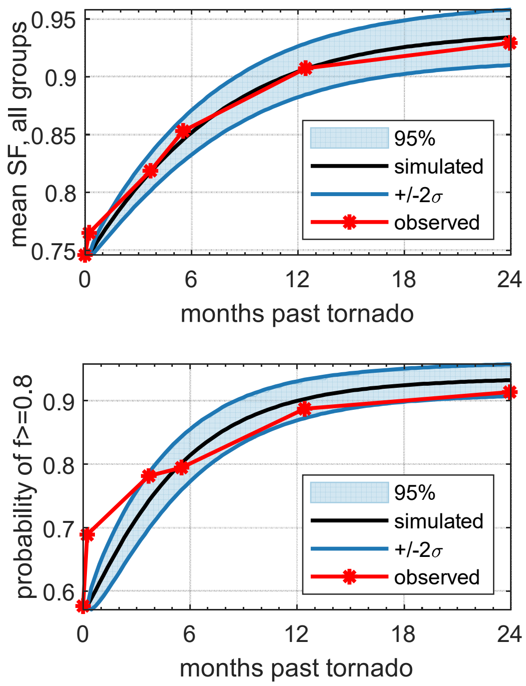

Fig. 9. Top: distribution of community mean recovery of structural functionality. Bottom: probability of usable structural functionality and observed proportion of usable buildings.

The probability that any building has structural functionality greater than or equal to SF 0.8 is a close approximation of the probability that the building structure and envelope are in a usable condition [6]. Fig. 9 (bottom) shows that the simulated recovery lags the observed recovery for this metric. The state-transition matrix recovery model allows for indeterminate recovery paths but does not provide state-transition probabilities that change with time. This model is a poor predictor of early rapid recovery of structural functionality possible with temporary repairs. The structural functionality indicators for wind-damaged structures allow for a rapid increase of $\Delta SF=0.1$ where temporary repairs are applied for envelope penetrations without structural damage [6].

Examining the mean recovery for all buildings grouped by post-event functionality (Fig. 10) reveals deeper trends in the data. The mean recovery of buildings with post-storm structural functionality above SF 0.3 has exponential-like behavior with rapid early recovery that asymptotically approaches a stable mean. Heavily damaged

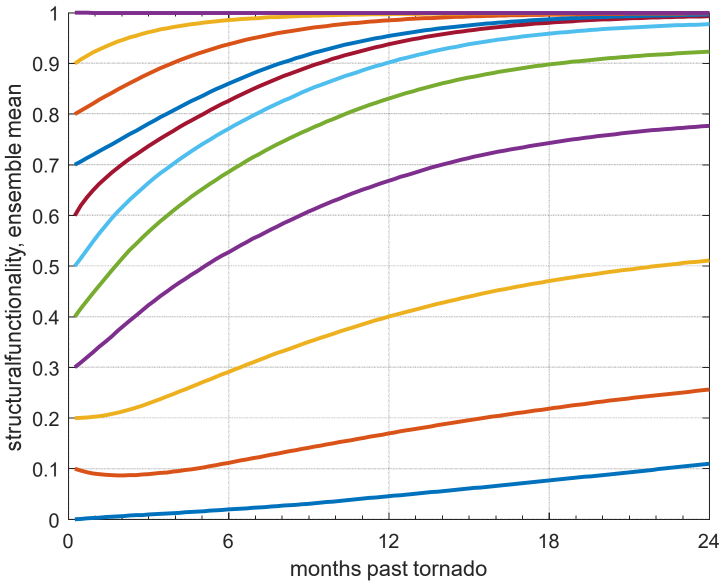

Fig. 10. Ensemble mean of simulated recovery by post-storm structural functionality.

buildings with post-storm structural functionality below SF 0.3 and above SF 0 have a mean recovery with an initial plateau or decrease in functionality — reflecting the reality that many buildings in this group must be fully or partially demolished before reconstruction begins. Buildings with post-storm structural functionality of SF 0.6 or greater recover to full structural functionality, on average. However, buildings with post-storm structural functionality below SF 0.6 recover to a stable mean structural functionality state below full structural functionality. The mean recovery of buildings with post-storm structural functionality SF 0 is relatively slow and nearly linear. This average trend toward structural functionality below SF 1 does not reflect the final structural functionality state for any individual building. An individual building may have any structural functionality, but observations suggest that most structures are either demolished (SF 0) or recover toward SF 1. This implies that the final mean structural functionality is similar to the proportion of buildings that fully recover. The advantage of using the eleven indicators of structural functionality for wind-damaged buildings (as opposed to lower-resolution systems with four or five discrete categories) is evident in Fig. 10: the difference in mean recovery behavior for buildings with post-storm functionality SF 0.2 and SF 0.3 would be obscured by a lower-resolution system, as would the wide gradient of mean final structural functionality observed in buildings with post storm functionality SF 0.3 to SF 0.6. Resilience models with damage indicators based on the damage states of HAZUS-MH would typically consider buildings with post-storm structural functionality below SF 0.4 as a monotonic group with total destruction [6, 20].

The simulated probabilities of usable structural functionality SF≥0.8 in Fig. 11 inherit the final structural functionality trends observed in Fig. 10, where buildings with lower post-storm structural functionality have some probability of not recovering to a usable state in the 2-year simulation period. Overall, buildings in a usable state after the storm passes maintain a usable state for the duration of the recovery period. Buildings with post-storm structural functionality below the SF 0.8 usable threshold have a very low probability of usability (near 0%) for a discrete period, then transition to a period of rapid increase in probability of usability before asymptotically approaching a stable final state.

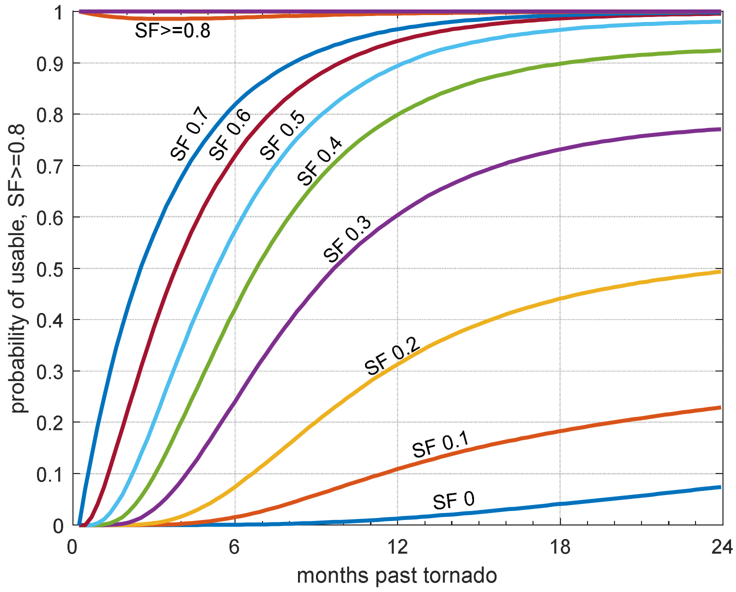

Fig. 11. Ensemble mean of simulated probability of usable structural functionality by post-storm structural functionality.

2.6 Deterministic Structural Functionality Recovery Models

Model Type	Lr	Lp	Tp	L

Deterministic recovery models cannot capture the variability in the recovery of individual buildings but are convenient for resilience analysis conducted without iterative simulations. Fitting standard recovery shape functions to the mean simulated recovery allows an approximation of the average recovery based on post-storm structural functionality.

Four deterministic recovery shapes are evaluated to describe the mean recovery for each post-storm structural functionality state: linear recovery (Eq. 2), exponential recovery (Eq. 3), trigonometric recovery (Eq. 4), and normal recovery (Eq. 5). The equations are adapted from Tokgoz and Gheorghe [9] for each recovery shape, adaptations include the addition of parameter L_P to model permanent loss in mean structural functionality.

$$SF_{lin}(t) = 1 - (L - L_P)\left(1 - \frac{L_R}{T_p}\, t\right) - L_P \leq 1 \tag{2}$$

$$SF_{exp}(t) = 1 - (L - L_P)(1 - L_R)^{\frac{t}{T_P}} - L_P \tag{3}$$

$$SF_{trig}(t) = 1 - (L - L_P) * \cos\left(\arccos(1 - L_R) * \frac{t}{T_P}\right) \leq 1 \tag{4}$$

$$SF_{norm}(t) = 1 - (L - L_P)(1 - L_R)^{\left(\frac{t}{T_P}\right)^2} - L_P \tag{5}$$

SF is the structural functionality, t is the time past the tornado in weeks, L is the initial loss, L_P is the permanent loss, T_P is an arbitrary evaluation time, and L_R is the percentage of the loss recovered at time $t=T_P$. All recovery functions are evaluated with T_P=52 weeks in this analysis.

All four functions are fit to the mean simulation recovery and the function with the lowest root-mean-square error for each post-storm structural functionality is selected as the optimal choice. Table 5 includes recommended model types and parameter values for each post-storm structural functionality. The values in Table 5 have been adjusted from the optimal fit values to reduce the number of significant digits and enforce decreasing L_R and increasing L_P with increasing L. The deterministic models provide a reasonable approximation of the mean simulated recovery (Fig. 12).

Post-storm functionality					
1	Linear/Constant	1.00	0	52	0.0
0.9	Exponential	0.98	0	52	0.1
0.8	Exponential	0.91	0	52	0.2
0.7	Exponential	0.83	0	52	0.3
0.6	Exponential	0.84	0	52	0.4
0.5	Exponential	0.81	0	52	0.5
0.4	Exponential	0.78	0.04	52	0.6
0.3	Exponential	0.68	0.16	52	0.7
0.2	Normal	0.65	0.48	52	0.8
0.1	Normal	0.30	0.68	52	0.9
0	Normal	0.30	0.85	52	1.0

Table 1. Deterministic mean recovery parameter

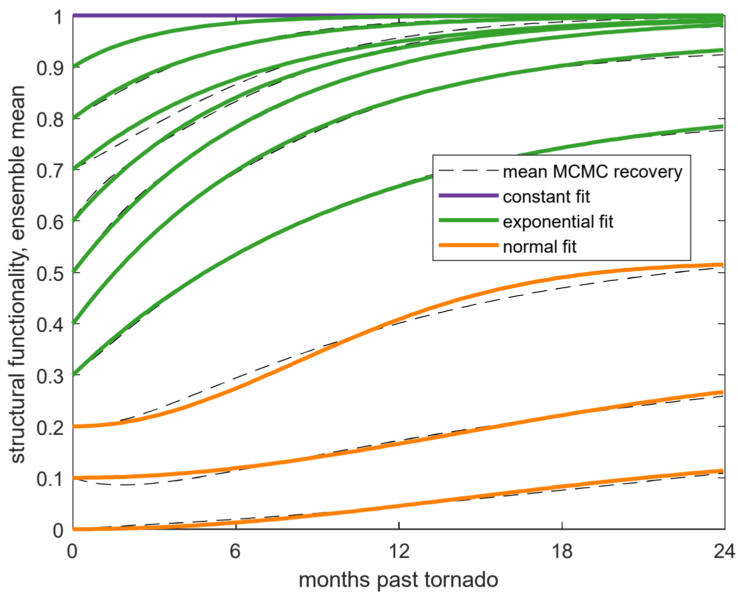

Fig. 12. Deterministic mean recovery functions with simulated mean recovery.

Binary recovery models, where a building is either usable or unusable, require probability that the structural functionality of the building is usable (SF≥0.8). None of the four recovery functions previously mentioned provide a reasonable fit for the probability of usable structural functionality SF≥0.8 (Fig. 11). Buildings with post-storm structural functionality SF≥0.8 are best modeled as having a constant 100% probability of being usable. A modified exponential fit with a lag before any increase in probability above 0% models the recovery of buildings with a post-storm structural functionality below SF 0.8 (Eq.6).

$$P(SF(t) \geq 0.8) = P_{INF} - P_{INF}(1 - P_R)^{\frac{t-T_{LAG}}{T_P}} \geq 0 \qquad (6)$$

P(SF(t)≥0.8) is the probability of the structural functionality state meeting the usability threshold, P_{INF} is the probability that a building is usable at t=infinity, P_R is the probability recovered at T_P, and T_{LAG} is the time in weeks before the probability increases above 0%. Table 6 summarizes the recommended function type and parameters for all post-storm structural functionality states. The values in Table 6 have been adjusted from the optimal fit values, primarily to reduce the number of significant digits. Models with lower post-storm functionality (SF=0 and SF=0.1) were adjusted to better approximate the lag behavior. Fig. 13 provides a comparison

Table 2. Deterministic probability of SF ≥ 0.8

Post-storm functionality	Fit Type	P_{INF}	P_R	T_{LAG}	T_P
1	Constant	1	NA	NA	NA
0.9	Constant	1	NA	NA	NA
0.8	Constant	1	NA	NA	NA
0.7	Lagged exp	1	0.97	0	52
0.6	Lagged exp	1	0.95	3	52
0.5	Lagged exp	0.99	0.93	7	52
0.4	Lagged exp	0.95	0.89	10	52
0.3	Lagged exp	0.82	0.83	14	52
0.2	Lagged exp	0.57	0.72	19	52
0.1	Lagged exp	0.35	0.51	23	52
0	Lagged exp	0.18	0.35	40	52

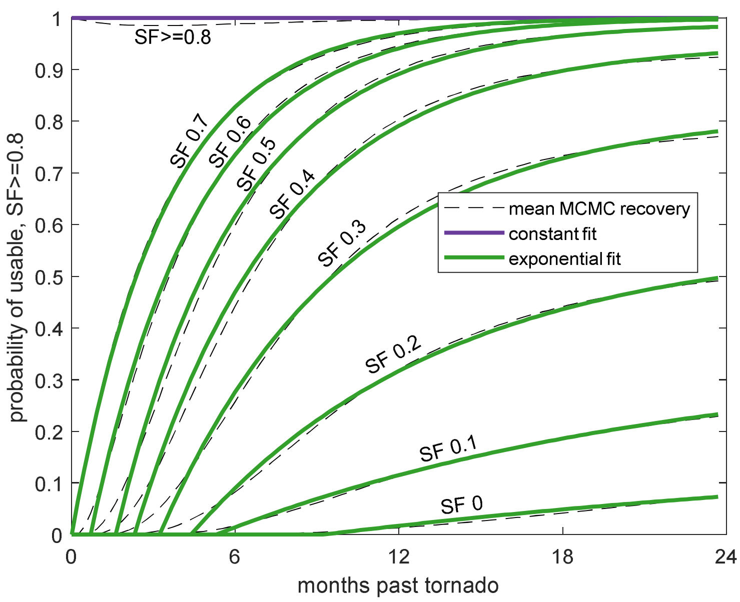

Fig. 13. Deterministic probability of SF ≥ 0.8 with simulated probability.

between the determinate probability functions and the mean simulated probability. This model underestimates the probability that a building is usable during the lag period for buildings with post-storm structural functionality between SF 0.1 and SF 0.6 but provides a reasonable estimate for most of the recovery period.

3. Application of the Structural Functionality Resilience Model

The empirical tornado resilience model for light-framed wood buildings developed above includes a set of damage models and recovery models designed to provide a complete description of structural functionality resilience and allow portability of the damage and recovery models to external resilience models. Structural functionality is one component of a building's total functionality: it describes the building's ability to safely serve as a shelter [6]. Any resilience model of total functionality must include structural functionality of buildings and the functionality of lifeline services (primarily transportation and utilities) and building services (such as temperature control). Lifeline services are community-scale systems and should not be modelled at the building level. The resilience of lifeline services has been extensively modeled elsewhere and is not reproduced here [30, 44-48].

As an independent model of building structural functionality resilience to tornado damage, the empirical tornado resilience model requires a set of peak wind speeds at each building as the sole input. Ideally, building geographic locations and either a historic or simulated tornado wind field yields the set of peak wind speeds. The structural functionality fragility model stochastically determines post-storm structural functionality from the set of peak wind speeds. Once the post-storm structural functionality is established, the structural functionality state recovery matrix stochastically determines the change in structural functionality for each building in a weekly simulation for any desired duration. In the observed recovery, most buildings reached a stable state of recovery after 2 years (105 weeks). The integral of the structural functionality over the simulation period yields the resilience of any building or group of buildings. Either fragility functions or direct application of the structural functionality scale (in physics-based models) can determine the post storm structural functionality in external resilience models. The conversions in Table 3 provide post-storm structural functionality where EF-Scale DOD fragilities are used. The appropriate choice of transition matrix, deterministic mean functionality functions, or deterministic probability of binary usability determine structural functionality recovery in external models. Robust total functionality resilience models should include provisions for secondary wind damage.

4. Conclusions

The empirical tornado resilience model for light-framed wood buildings developed herein is an observation-based resilience model for residential buildings subject to tornado damage. The resilience model includes the components below, filling the research need for observations of residential recovery, tornado functionality fragility and recovery descriptions, and bases for validation of existing and future conceptual models.

(1) An empirical fragility model for structural functionality states SF 0.4 through SF 1 based on data collected in Naplate, IL. The fairly even spacing of the well-defined fragility curves may suggest that the structural functionality indicators for wind-damaged structures provide an even meter of progressive damage.

(2) Probabilities of post-storm structural functionality based on EF-Scale DOD, enabling use of the structural functionality scale with fragility models for EF-Scale DOD. These

probabilities also enable resilience analysis based on existing datasets from ground surveys following tornado damage that include EF-Scale DOD ratings and estimated wind speeds.

(3) A structural functionality transition matrix recovery model that provides building-level recovery paths in an iterative recovery simulation. Comparisons between simulation runs from the state-transition matrix and recovery observations in Naplate, IL suggest that the transition matrix is a possible parent model for the observations. This recovery model allows incremental increases and decreases in functionality — matching the observation that some structures are demolished/partially demolished during recovery. The structural functionality scale indicators for windstorm damage provide a higher resolution of progressive losses in functionality than typically included in resilience analysis. The higher resolution reveals differences in behavior that would not otherwise be discernable, particularly the tail behavior observed in recovery of heavily damaged buildings (Fig. 7) and difference in mean recovery shape for buildings with initial structural functionality SF=0.2 and SF=0.3 (Fig. 10).

(4) Deterministic recovery models for mean structural functionality and probability of usable structural functionality. The deterministic models do not provide unique recovery paths for individual buildings but may be easily adapted to different regions where market pressures control the permanent loss in mean functionality. The exponential recovery function is appropriate to describe the mean recovery of building with most levels of damage; the mean recovery of heavily damaged buildings is best described with normal/s-shaped recovery. A new formulation for delayed exponential recovery is introduced as the best model for binary useable/not usable structural functionality

resilience for all buildings with sufficient damage to not be usable (post-storm functionality below SF=0.8). The advantage inherent in using the higher-resolution structural functionality scale is also clear in the deterministic models where buildings with different levels of damage that would be indistinguishable in lower-resolution classification, such as damage states based on HAZUS-MH, show significantly different tail behavior (final mean structural functionality) and different mean recovery curve shape (Fig. 12 and Fig. 13).

(5) A basic framework for implementing the fragility and recovery models as an independent resilience model or integrating both/either into resilience models with measures of other functionality components.

Overall, the empirical resilience model addresses the need to quantify the recovery of light-framed wood residential buildings. The components of the empirical resilience model naturally include the effects of socioeconomic influences and individual owner decision criteria, but do not explicitly account for these factors. Field observations of damage and recovery and the structural functionality scale for light-framed wood buildings are the basis for this empirical model. The structural functionality scale measures the ability of a building to safely provide shelter and includes considerations of the structural system and building envelope: it does not account for the functionality of lifeline services or building services. When combined with a lifeline systems model, this building-level detail allows consideration of how lifeline system policy could be optimized to provide services to buildings which are more likely to have a useable structural functionality state.

Without extrapolation, this model can only be directly applied to simulations where the maximum wind speed is below 60 m/s and the residential buildings in the study are typical light-framed wood construction built without any improved wind-resisting components such as rafter ties. The observation set includes residences with unreinforced masonry foundation walls which are still commonly used in noncoastal regions where code/enforcement does not require reinforcement. Use of the recovery model in a simulation with higher wind speeds is reasonable when coupled with a damage model that measures functionality using the structural functionality scale. Given the limitations of data from a single community, additional observations of light-framed wood residential buildings built with standard construction and separate residential buildings with improvements that increase resilience (e.g. rafter ties, improved wall anchorage, improved sheathing fasteners) would be required to build an empirical model with the ability to quantify resulting improvements in resilience — this evaluation is beyond the scope of the current dataset. The size of the sample set has unavoidable implications on the uncertainty of the transition matrix (Table 4); for each of the 11 discrete functionality states (SF=0 to SF=1 at ΔSF=0.1) the total number of buildings that transitioned from that state is 916, 133, 145, 63, 67, 97, 140, 781, 1089, 1157, and 11156, respectively. The total number of transitions (15744) is about 2.5% higher than the product of buildings and transition weeks (151 buildings @ 104 transitions) because the process for dividing the dwell time of interpolated states was designed for even distribution instead count preservation (the rounding process has a positive bias).

The empirical resilience model has the additional potential to calibrate or validate existing and future conceptual models. The observed and simulated recovery behavior also provide guidance for the development of analytical models by showing the true shape of recovery for light-framed wood buildings subject to tornado damage. Ideally, future field studies will illuminate the effects of public policy and socioeconomic influences that are not revealed with data from a single location or event.

Acknowledgements

This project was funded in part by NOAA VORTEX-SE grant NA16OAR4590219. Daniel Rhee, Antonio Zaldivar, Guangzhao Chen, Alexander Zickar, Rishabh Moorjani, Amanda R. Lombardo, and Jennifer Vertrone all contributed to the field campaign surveying the recovery of Naplate, IL following tornado damage on 28 February 2017.

References

1. Bonstrom, H. and R.B. Corotis, *First-Order Reliability Approach to Quantify and Improve Building Portfolio Resilience.* Journal of Structural Engineering, 2016. **142**(8): p. C4014001.
2. Koliou, M., et al., *State of the research in community resilience: progress and challenges.* Sustainable and Resilient Infrastructure, 2018.
3. van de Lindt, J., B. Ellingwood, and T. McAllister, *Structural Design and Robustness for Community Resilience to Natural Hazards.* Journal of Structural Engineering, 2020. **146**(1).
4. Mieler, M. and J. Mitrani-Reiser, *Review of the state of the art in assessing earthquake-induced loss of functionality in buildings.* Journal of Structural Engineering, 2017. **144**(3): p. 04017218.
5. McAllister, T., *NIST Technical Note 1795: Developing Guidelines and Standards for Disaster Resilience of the Built Environment: A Research Needs Assessment*, U.S.D.o.C. National Institute of Standards and Technology, Editor. 2013.
6. Nevill, J.B. and F.T. Lombardo, *Structural functionality scale for light-framed wood buildings with indicators for windstorm damage.* Journal of Structural Engineering, 2020. **164**(4).
7. Bruneau, M., et al., *A framework to quantitatively assess and enhance the seismic resilience of communities.* Earthquake Spectra, 2003. **19**(4): p. 733-752.

8. Cimellaro, G., A. Reinhorn, and M. Bruneau, *Framework for analytical quantification of disaster resilience.* Engineering Structures, 2010. **32**(11): p. 3639-3649.

9. Tokgoz, B. and A. Gheorghe, *Resilience Quantification and Its Application to a Residential Building Subject to Hurricane Winds.* International Journal of Disaster Risk Science, 2013. **4**(3): p. 105-114.

10. Nocera, F., P. Gardoni, and G. Cimellaro, *Time-Dependent Probability of Exceeding a Target Level of Recovery.* Asce-Asme Journal of Risk and Uncertainty in Engineering Systems Part a-Civil Engineering, 2019. **5**(4).

11. Lin, P. and N. Wang, *Stochastic post-disaster functionality recovery of community building portfolios I: Modeling.* 2017.

12. Bevington, J.S., et al., *Measuring, Monitoring and Evaluating Post-Disaster Recovery: A Key Element in Understanding Community Resilience*, in *Structures Congress 2011*, D. Ames, T.L. Droessler, and M. Hoit, Editors. 2011, ASCE Press: Las Vegas, Nevada. p. 2033-2043.

13. Hassan, E. and H. Mahmoud, *A framework for estimating immediate interdependent functionality reduction of a steel hospital following a seismic event.* Engineering Structures, 2018. **168**: p. 669-683.

14. Cimellaro, G., A. Reinhorn, and M. Bruneau, *Seismic resilience of a hospital system.* Structure and Infrastructure Engineering, 2010. **6**(1-2): p. 127-144.

15. Cimellaro, G., A. Reinhorn, and M. Bruneau, *Performance-based metamodel for healthcare facilities.* Earthquake Engineering & Structural Dynamics, 2011. **40**(11): p. 1197-1217.

16. Miles, S. and S. Chang, *ResilUS: A Community Based Disaster Resilience Model.* Cartography and Geographic Information Science, 2011. **38**(1): p. 36-51.

17. Zhang, Y. and W. Peacock, *Planning for Housing Recovery? Lessons Learned From Hurricane Andrew.* Journal of the American Planning Association, 2009. **76**(1): p. 5-24.

18. Sutley, E. and S. Hamideh, *An interdisciplinary system dynamics model for post-disaster housing recovery.* Sustainable and Resilient Infrastructure, 2018. **3**(3): p. 109-127.

19. Rojah, C., *ATC-20-1 Field Manual: Postearthquake Safety Evaluation of Buildings.* 2005.

20. Vickery, P., et al., *HAZUS-MH hurricane model methodology. II: Damage and loss estimation.* 2006.

21. FEMA, *Multi-hazard Loss Estimation Methodology: Hurricane Model; Hazus-MH 2.1 Technical Manual*, H. Security, Editor. 2011, Federal Emergency Management Agency.

22. Dong, Y. and Y. Li, *Risk Assessment in Quantification of Hurricane Resilience of Residential Communities.* Asce-Asme Journal of Risk and Uncertainty in Engineering Systems Part a-Civil Engineering, 2017b. **3**(4).

23. Attary, N., et al., *Hindcasting community-level building damage for the 2011 Joplin EF5 tornado.* Natural Hazards, 2018. **93**(3): p. 1295-1316.

24. Masoomi, H., M. Ameri, and J. van de Lindt, *Wind Performance Enhancement Strategies for Residential Wood-Frame Buildings.* Journal of Performance of Constructed Facilities, 2018. **32**(3).

25. Zhao, D., A. McCoy, and J. Smoke, *Resilient Built Environment: New Framework for Assessing the Residential Construction Market.* Journal of Architectural Engineering, 2015. **21**(4).

26. Dong, Y. and Y. Li, *Evaluation of Hurricane Resilience of Residential Community Considering a Changing Climate, Social Disruption Cost, and Environmental Impact.* Journal of Architectural Engineering, 2017. **23**(3).

27. Wang, N. and B.R. Ellingwood, *Disaggregating Community Resilience Objectives to Achieve Building Performance Goals*, in *12th International Conference on Applications of Statistics and Probability in Civil Engineering, ICASP12*. 2015, University of British Columbia: Vancouver, Canada.

28. Disasters), C.C.f.R.o.t.E.o., *Economic losses, poverty & disasters 1998–2017*. 2018, CRED: Brussels, Belgium.

29. Lombardo, F., *Engineering Analysis of a Full-Scale High-Resolution Tornado Wind Speed Record.* Journal of Structural Engineering, 2018. **144**(2).

30. Memari, M., et al., *Minimal Building Fragility Portfolio for Damage Assessment of Communities Subjected to Tornadoes.* Journal of Structural Engineering, 2018. **144**(7).

31. Masoomi, H. and J. van de Lindt, *Restoration and functionality assessment of a community subjected to tornado hazard.* Structure and Infrastructure Engineering, 2018. **14**(3): p. 275-291.

32. Ellingwood, B., et al., *Fragility assessment of light-frame wood construction subjected to wind and earthquake hazards.* Journal of Structural Engineering-Asce, 2004. **130**(12): p. 1921-1930.

33. Maloney, T., et al., *Performance and risk to light-framed wood residential buildings subjected to tornadoes.* Structural Safety, 2018. **70**: p. 35-47.

34. Roueche, D., F. Lombardo, and D. Prevatt, *Empirical Approach to Evaluating the Tornado Fragility of Residential Structures.* Journal of Structural Engineering, 2017. **143**(9).

35. Roueche, D., D. Prevatt, and F. Lombardo, *Epistemic Uncertainties in Fragility Functions Derived from Post-Disaster Damage Assessments.* Asce-Asme Journal of Risk and Uncertainty in Engineering Systems Part a-Civil Engineering, 2018. **4**(2).

36. van de Lindt, J.W., et al., *Validating Interdependent Community Resilience Modeling using Hindcasting*, in *13th International Conference on Applications of Statistics and Probability in Civil Engineering, ICASP13*. 2019, S-Space, Seoul National University: Seoul, South Korea.

37. Koliou, M. and J. van de Lindt, *Development of Building Restoration Functions for Use in Community Recovery Planning to Tornadoes.* Natural Hazards Review, 2020. **21**(2).

38. Attary, N., et al., *Hindcasting Community-Level Damage to the Interdependent Buildings and Electric Power Network after the 2011 Joplin, Missouri, Tornado.* Natural Hazards Review, 2019. **20**(1).

39. Wind Science and Engineering Center, *A Recommendation for an Enhanced Fujita Scale (EF-Scale).* 2006, Texas Tech University: Lubbock, TX.

40. National Weather Service. *February 28, 2017: Tornado Event*. 2019 August 20th 2019 1:34 PM; Available from: https://www.weather.gov/lot/2017Feb28_tornadoes.

41. Rhee, D. and F. Lombardo, *Improved near-surface wind speed characterization using damage patterns.* Journal of Wind Engineering and Industrial Aerodynamics, 2018. **180**: p. 288-297.

42. Lallemant, D., A. Kiremidjian, and H. Burton, *Statistical procedures for developing earthquake damage fragility curves.* Earthquake Engineering & Structural Dynamics, 2015. **44**(9): p. 1373-1389.

43. Godfrey, C. and C. Peterson, *Estimating Enhanced Fujita Scale Levels Based on Forest Damage Severity.* Weather and Forecasting, 2017. **32**(1): p. 243-252.

44. Donovan, B. and D.B. Work, *Empirically quantifying city-scale transportation system resilience to extreme events.* Transportation Research Part C: Emerging Technologies, 2017. **79**: p. 333-346.

45. Guidotti, R., et al., *Modeling the resilience of critical infrastructure: the role of network dependencies.* Sustainable and Resilient Infrastructure, 2016. **1**(3-4): p. 153-168.

46. Koliou, M., H. Masoomi, and J. van de Lindt, *Performance Assessment of Tilt-Up Big-Box Buildings Subjected to Extreme Hazards: Tornadoes and Earthquakes.* Journal of Performance of Constructed Facilities, 2017. **31**(5).

47. Mensah, A. and L. Duenas-Osorio, *Efficient Resilience Assessment Framework for Electric Power Systems Affected by Hurricane Events.* Journal of Structural Engineering, 2016. **142**(8).

48. Ramachandran, V., et al., *Framework for Modeling Urban Restoration Resilience Time in the Aftermath of an Extreme Event.* Natural Hazards Review, 2015. **16**(4).